Research Report

DEVELOPMENT OF A TRUCK MOUNTED ATTENUATOR

Submitted to

GP Sp. z o. o.

Prepared by

Andrzej S. Nowak, Ph.D.,

DECEMBER 2015

1. Report No. G00008268	**2. Government Accession No.**	**3. Recipient Catalog No.**
4 Title and Subtitle DEVELOPMENT OF A TRUCK MOUNTED ATTENUATOR		**5 Report Date** December 2015 **6 Performing Organization Code**
7. Author(s) Andrzej S. Nowak		**8 Performing** G00008268
9 Performing Organization Name and Address Department of Civil Engineering 238 Harbert Engineering Center Auburn, AL 36849		**10 Work Unit No. (TRAIS)** **11 Contract or Grant No.**
12 Sponsoring Agency Name and Address GP Sp. z o.o. ul. Struga 80A 70-784 Szczecin, Poland		**13 Type of Report and Period Covered** Technical Report **14 Sponsoring Agency Code**

15 Supplementary Notes

16 Abstract

Roadside safety is one of the major research areas in engineering. Truck Mounted Attenuators are used to protect motorists, workers, and equipment from road accidents. Usually they consist of an energy absorption cushion and lift up unit called the docking station which is used for mobile carrier attachment. In case of collision, these safety devices must dissipate kinetic energy in a satisfactory manner such that the deceleration does not exceed critical levels for the drivers and passengers. The objective of this research project is to develop a new truck mounted attenuator designated for 100 [km/h]. Multiple crash test were performed including rigid bogie and real vehicles choose according to design standards cars. The collected test data was used to calibrate the finite element model in order to optimize the structure.

17 Key Words Truck Mounted Attenuator, MASH Design, NCHRP 350 Design, EN1317 Design, Nonlinear Impact Analysis.		**18 Distribution Statement** Restricted – Sponsoring Company Only	
19 Security Classification (of this report) Unclassified	**20 Security Classification (of this page)** Unclassified	**21 No. of pages** 172	**22 Price**

Research Report

Research Project #G00008268

DEVELOPMENT OF A TRUCK MOUNTED ATTENUATOR

Submitted to

GP Sp. z o. o.

Prepared by

Andrzej S. Nowak, Ph.D.

Department of Civil Engineering at

Auburn University

DECEMBER 2015

DISCLAIMERS

The contents of this report reflect the views of the authors, who are responsible for the facts and the accuracy of the data presented herein. The contents do not necessarily reflect the official views or policies of Auburn University. This report does not constitute a standard, specification, or regulation.

NOT INTENDED FOR CONSTRUCTION, BIDDING, OR PERMIT PURPOSES

Andrzej S. Nowak, Ph.D.
Research Supervisor

ABSTRACT

Roadside safety is one of the major research areas in engineering. Truck Mounted Attenuators are used to protect motorists, workers, and equipment from road accidents. Usually they consist of an energy absorption cushion and lift up unit called the docking station which is used for mobile carrier attachment. In case of collision, these safety devices must dissipate kinetic energy in a satisfactory manner such that the deceleration does not exceed critical levels for the drivers and passengers. The objective of this research project is to develop a new truck mounted attenuator designated for 100 [km/h]. Multiple crash test were performed including rigid bogie and real vehicles choose according to design standards cars. The collected test data was used to calibrate the finite element model in order to optimize the structure.

TABLE OF CONTENTS

LIST OF FIGURES

LIST OF TABLES

CHAPTER 1. INTRODUCTION

1.1. Problem Statement

Road safety is a very important issue as it affects millions of people. Although the safety measures implemented so far have been effective, the number of road fatalities is unacceptably high. There is an urgent need for improvement in Europe, North America and the rest of the world. The main reasons for a high mortality rate are: poor quality of the roads, technical condition of the vehicles, and improper driver behavior (speeding, driving under the influence of alcohol, drugs or tiredness, lack of seat belts, riding without a helmet, etc.).

Globally on the roads, due to different types of accidents and collisions about 1.2 million people are killed every year, and this is equivalent to a new fully loaded Boeing 787 crashing every two hours. In addition, every year 50 million people are seriously injured in traffic crashes.

Figure. 1.1. Example of Truck Mounted Attenuator (http://huddig.se).

Many fatalities and sever injuries can be prevented by road-side safety devices such as a Truck Mounted Attenuator((TMA), which is the object of this research project. TMA's are used to protect motorists, workers, and equipment from serious consequences road accidents. A typical attenuator consists of an energy absorption cushion mounted on a truck and a unit called docking station. This unit provides a connection between the attenuator and truck and it also lifts up the energy absorption cushion for transportation. During impact, the cushion must dissipate the kinetic energy in such a way that the deceleration does not exceed critical levels for the drivers and passengers.

From the theoretical point of view, the development of a truck mounted attenuator requires estimation of the energy dissipation levels by combining the basic principles of physics and critical mechanical effects for people.

The major problem in the design of structural elements is the development of cross section of main components and be properly assigned along the cushion length, so the energy can be dissipated in the desired manner. To accomplish this two different approaches can be used:

- **Trial-and-error Approach Method**, which involves numerous field tests that are very expensive.

- **Finite Element Method (FEM)**, which is effective numerical procedure to find the solution for various engineering problems. Recently, FEM is even more powerful due to an increased computational power.

1.2. Objective And Scope Of The Research Project

The main objective of this research project is to develop a truck mounted attenuator with a capacity to absorb energy and stop a vehicles traveling with speed up to 100 km/h.

In this research, multiple nonlinear finite element models were developed using the commercial software ABAQUS and LS-Dyna. Computer simulations can significantly reduce the number of expensive full-scale crash tests that are otherwise required for the development of the system.

Based on acquired information from analytical and numerical analysis combined with field testing, the truck mounted attenuator was optimized to meet all of the required criteria.

1.3. Prior Investigations

Research on the development of a truck mounted attenuator and related with it finite element modeling is not well documented in the available literature with only sporadic documents available. This is partly due to fact that the final products are protected by patents and none of the companies are interested in revealing their designs. Hence, the procedures describing the development of such a structure were never published. On the other hand, patents have to be checked prior to starting the design to avoid the situations where implementation of a specific detail can be protected by the patent law.

Literature available for this study can be divided into two main groups: one corresponding to the numerical analysis and the other one related to the design criteria.

Carney et al. [9] in his research paper described the development of a crash cushion made from polyethylene cylinders using finite-element modeling by DYNA3D software. Belingardi and Obradovic [8] used a numerical procedure to optimize values of kinematic energy dissipation in order to control deceleration during the impact. Only these two papers considered the problem that is very close to the objective of this study. However, the documentation included with ABAQUS Unified FEA and LS-Dyna software was the most useful. It contains multiple validated numerical examples for static and dynamic problems with precise description of various modeling techniques including a theoretical background.

There are also numerous reports from the United States Department of Transportation that provide information about the behavior of truck mounted attenuators that are available on the market. In addition, they describe the testing procedures that are used as serviceability criteria. Most importantly, they describe the requirements from the current design codes available in United States of America: NCHRP Report 350 [6] or Manual for Assessing Safety Hardware [5] and European Norm that defines common testing and certification procedures for road restraint systems [4].

CHAPTER 2. DESIGN PARAMETERS AND ACCEPTABILITY CRITERIA

2.1. General

A designed structure has to satisfy many criteria, so that the final product can serve well over its intended lifetime. A economic lifetime of five years is assumed. Therefore, the attenuator has to be capable of safely stopping vehicles with a velocity of 100 km/h or less within a five year time frame. The important safety requirements are the critical occupant impact velocity (OIV) and occupant ride down deceleration (ORD), that should not exceed 20 g, while serviceability is conditioned primarily by a fatigue problem caused by vibrations.

Moreover, this study is concerned with truck mounted attenuators that would obtain certificates available both in the United States of America and European Union. Therefore, a design is based on the draft of a new EN 1317 Road Restraint Systems [4] and NCHRP Report 350: Recommended Procedures for the Safety Performance Evaluation of Highway Features [6] or AASHTO's Manual for Assessing Safety Hardware [5]. The adopted approach is first for the cushion to pass the test required in North America and then the additional tests required by the European code. A brief summary of the test conditions for each code are presented in Tables 2.1 – 2.4.

Test Level	Test Designation	Type of vehicle	Impact conditions	
			Test Mass [kg]	Speed [km/h]
3	3-50	passenger car	820	100
	3-51 to 3-53	pickup truck	2000	100

Table 2.1 - TMA test conditions based on NCHRP Report 350 [6].

Speed Class	Test Designation		Car	
			Total Test Mass [kg]	Impact Speed [km/h]
100	TL 100	100-2a	1300	100
		100-2b	1500	100

Table 2.2 - Additional conditions based on draft of new EN 1317 [4] for TMA's tested on NCHRP 350 [6].

Test Level	Test Designation	Type of vehicle	Impact conditions	
			Test Mass [kg]	Speed [km/h]
3	50	passenger car	1100	100
	51-53	pickup truck	2270	100

Table 2.3 - TMA's test conditions based on MASH [5].

Speed Class	Test Designation		Car	
			Total Test Mass [kg]	Impact Speed [km/h]
100	TL 100	100-1	900	100
		100-2a	1300	100
		100-2b	1500	100

Table 2.4 - Additional conditions based on draft of new EN 1317 [4] for TMA's tested on MASH [5].

The above tables do not provide the applicable approach angle or specified location of the impact, e.g. head on center, and properties of the truck. For more details please refer to specified reports.

Extended discussion regarding the aforementioned criteria can be found further in this chapter.

2.2. Occupant Risk

The design approach considers a hypothetical occupant who is unrestrained on the front seat. During the impact, the occupant's motion is dependent upon the vehicle's deceleration. The occupant can move within the vehicle space. Over the considered period of time, the forces acting

on the vehicle are not transferred to the driver. However, at some point in time, the occupant strikes a hypothetical element of car's interior, e.g. windshield, steering wheel, etc. From that point in time, by contact, the occupant begins to suffer the same forces as decelerating vehicle.

Two criteria have to be considered:

Longitudinal and lateral components of occupant velocity at impact with interior surface.

Highest lateral and longitudinal components of resultant occupant deceleration force at every 10 msec intervals.

Critical values based on NCHRP Report 350 [6] can be found in Tables 2.5 -2.6.

Component	Preferred value [m/s]	Maximum value [m/s]
Longitudinal and Lateral	9	12
Longitudinal	3	5

Table 2.5 - Occupant impact velocities limits for NCHRP 350 [6].

Component	Preferred value [g]	Maximum value [g]
Longitudinal and Lateral	15	20

Table 2.6 - Occupant ride down deceleration limits for NCHRP 350 [6].

2.2.1. Ride Down Deceleration

Deceleration is a negative acceleration that appears whenever a body in a motion starts slowing down. So the rate at which velocity of a body change within the time has minus sign and acceleration is described by Newton's second Law.

$$F = ma \tag{2.1}$$

$$a = \frac{\Delta v}{\Delta t} \tag{2.2}$$

Where: F is force, m is a body mass, a defines the acceleration or deceleration, Δv and Δt are change in velocity and time.

Velocity alone is not dangerous for occupant's safety. The only problem lies in period of time over which it changes. In general, high values of acceleration or deceleration will not necessarily result in serious injuries. What can be critical is a high magnitude within a certain time interval. Human body is composed of different organs and each organ has a given density. As a result, body parts with a higher density cause certain organs are subjected to higher gravity forces than other organs. Hence, a high acceleration of these organs, e.g. the brain, lungs, ribs (any bones), can affect the damage done to the human body.

Some levels of acceleration force that can be found in the real world are presented below:

- roller coaster rides can produce forces of maximum 3 to 4 [g];
- blackout or death can occur whenever force of 4 to 6 g is kept for more than a few seconds;
- crash of Princess Diana of Wales in 1997 was in a range of between 70 to 100g;
- biomechanics engineers and automotive researchers assume that human head can take about 80 g for several milliseconds without injury and the chest can stand about 60 g but only if the force is uniformly distributed;

- pilots in jetfighters can be subjected to 9 g in evasive maneuvers. Such a high amount of gravitational force take blood and oxygen away from the brain, heart and lungs resulting in fatigue, blackouts, or even death.

There are ways to control the acceleration force. The best approach to achieve a success without exceeding the limiting values is by controlling the stopping distance. This can be easily estimated using basic laws of physics. For more information refer to Chapter 4.

2.2.2. Impact Velocity

During the impact, the vehicle starts to rapidly decelerate. At that point the unrestrained occupant still moves at the pre-collision velocity until he/she impacts the interior features and fixtures. In a case when one part of the body is accelerated, then we can expect that the whole body will start rotating, resulting in a change of impact trajectory. The occupant will then undergo several impacts to various parts of his/her body until final post-collision position is achieved.

In the automotive industry, the main effort is put to reducing the risk of occupant's injury during a collision by decreasing the relative velocity between the occupants and the vehicle interior. Still large distances between occupant and the car's interior are required to stop the vehicles from high velocities and sustain sub-injury levels for occupant. Modern vehicles are equipped with many restrain systems such as safety belts, air bags, or more advance energy absorption systems, such as collapsible steering column or knee bolsters. Proper combination of the above elements can significantly increase this distance.

The speed at which the occupant hits the interior components may be different from the speed change of vehicle if various restrain systems are used. This differences are illustrated on Figures 2.1-2.2.

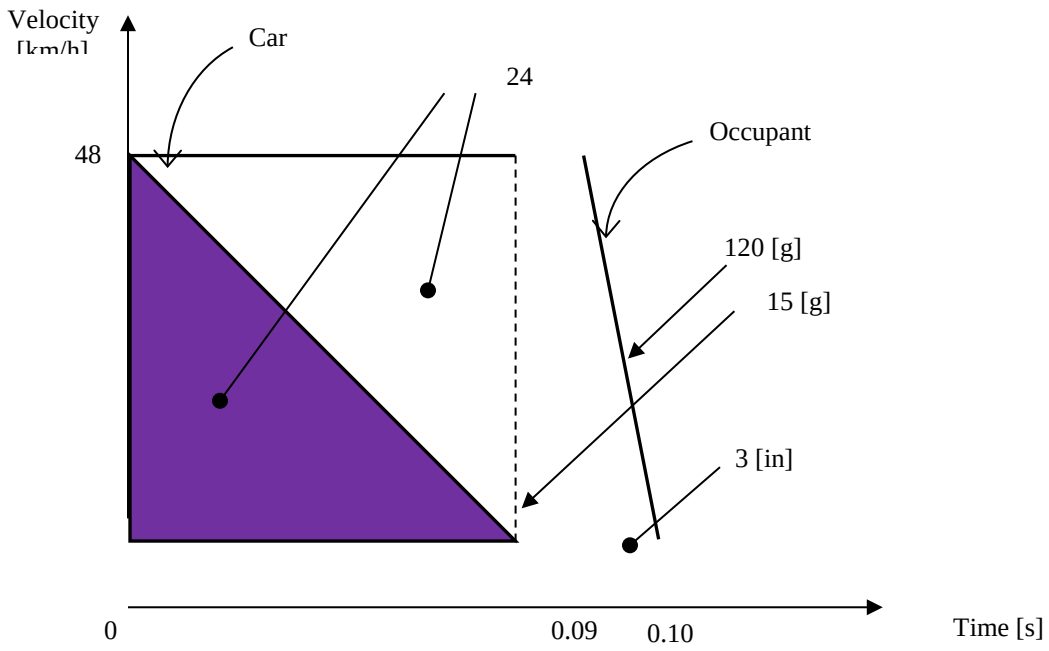

Figure. 2.1. Velocity-time diagram of crashing vehicle with rigid barrier for unrestrained occupant [18].

Due to the restraint system the occupant's speed will decrease in a gentler way. This will result in smaller deceleration values which are more preferred. Hence, whenever a modern vehicle impacts a truck mounted attenuator and it is equipped with multiple restraint systems, then safer forces will be experienced by the driver and passengers.

A theoretical approach which was used in occupant impact velocity estimation for TMA is described further in text. It is based on a flail-space approach.

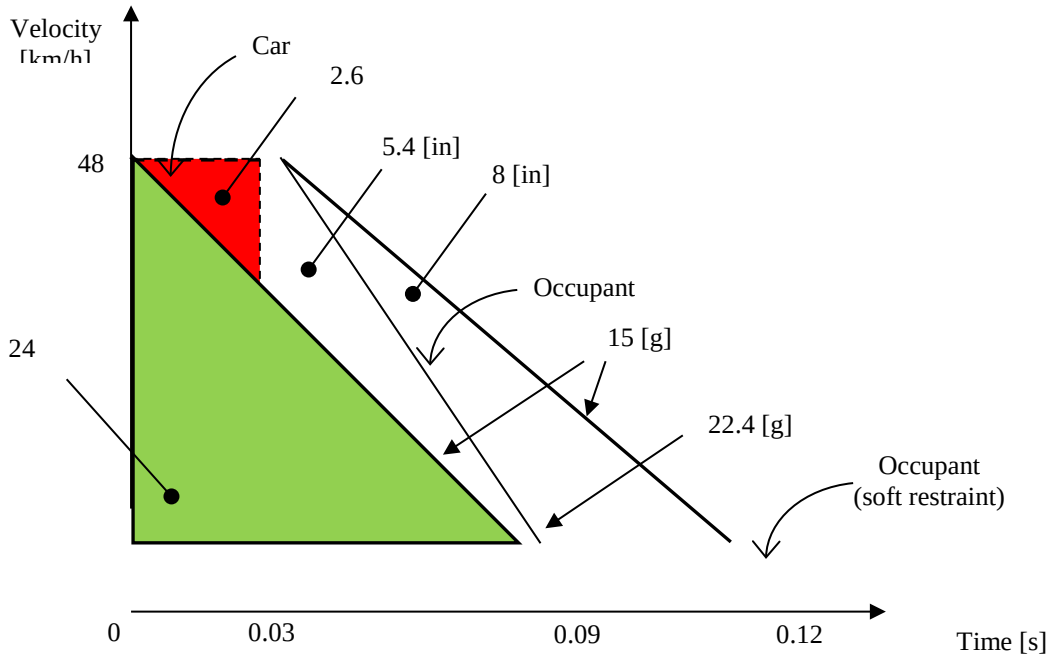

Figure. 2.2. Velocity-time diagram of crashing vehicle with rigid barrier for restrained driver [18].

2.2.3. Flail-Space Approach

The expression for the occupant impact velocity is given by:

$$OIV_{x,y} = \int_0^{t^*} a_{x,y} dt \tag{2.3}$$

where $OIV_{x,y}$ is occupant impact velocity in x or y directions, $a_{x,y}$ vehicular acceleration in x or y directions, t^* correspond to the time when occupant has traveled 0.6[m] (24 [in]) on x direction or 0.3[m] (12 [in]) on a y direction

t^* time can be estimated based on incremental integration

$$t^* = \min[t^*_x, t^*_y] \tag{2.4}$$

$$X = \iint_0^{t^*_x} a_x dt^2 \tag{2.5}$$

$$Y = \iint_0^{t^*_y} a_y dt^2 \tag{2.6}$$

Where: X correspond to longitudinal direction and it is equal to 0.6 [m] (24 [in]) and Y describes lateral direction and it is assumed as 0.3 [m] (12 [in]).

Since the model assumes that the occupant will not touch the interior before t^* then occupant ride down deceleration should be estimated after $t^* + 0.005$ [s].

2.3. Fatigue Test

Truck mounted attenuators are subjected to multiple vibrations over its lifetime. If this issue has not been considered in the design procedure, then structural failure could appear even within a small amount of time after being placed into service. Moreover, the safety benefits could be affected too.

Trucks with attenuator will travel most of the distance on primary and secondary roads. Construction zones will occur very rarely. Hence, TMA's are subjected to many different frequencies. When a cushion vibrates, then the structural elements will respond in a manner that depends upon the ratio between imposed and natural frequency. Those members are the truck, attenuator itself or docking station that connects the attenuator with truck, etc. It is well known that

higher displacement amplitudes are achieved when the component's vibrations are closer to its natural frequency.

Selection of the right range is very crucial to determining if the cushion is able to withstand the field hardness for many years. 2 [Hz] cannot be consider for TMA system because it corresponds to truck suspension. Across the United States of America, many different procedures are available. For this study, a procedure described by California Department of Transportation is assumed to be used in the design process and implemented in a finite element analysis. Results are compared with SN curves provided in Design Manual for Steel and Aluminum to estimate the lifetime.

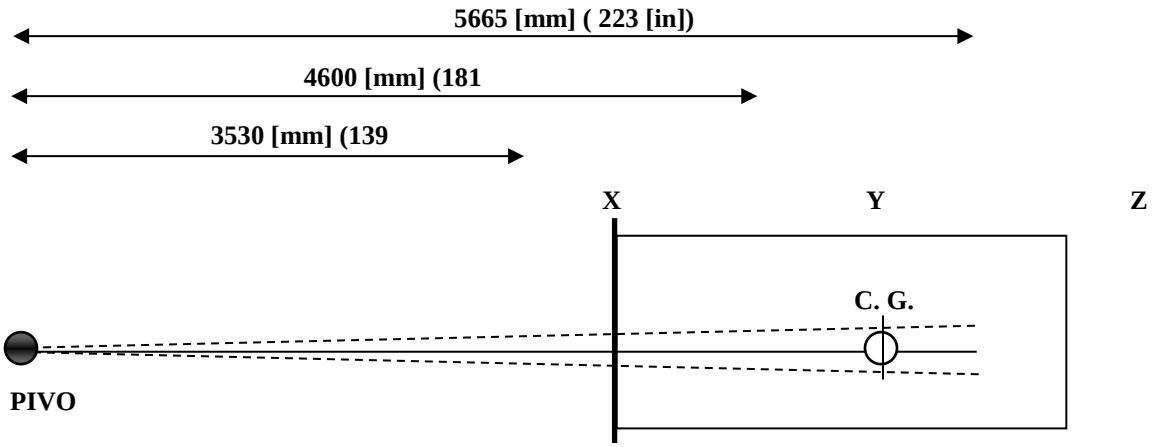

Figure. 2.3. Schematic drawing of the California Vibration Test Apparatus at 6 [Hz] [7].

California department of Transportation uses an accelerated fatigue test only on isolated TMA mounted on the arm of 139 [in] (3530 [mm]). Tests are conducted in three different positions:

horizontal (0^o), at an angle of 60^o and vertical (90^o). Frequency is described by a sinusoidal curve that varies between 6 to 8 [Hz]. Moreover, constant peak to peak amplitude of 0.6 [in] (15 [mm]) is assumed. The force on the tester can be described by below formula:

$$a = 4\pi^2 f^2 A \tag{2.7}$$

Where: A is a peak displacement, a is peak acceleration and f correspond to vibration frequency. Severity of the test is measure as a maximum of the vertical acceleration at the mounting plate. Using the above equation and prescribed conditions, this acceleration varies from $\pm$ 1.1 [g] to $\pm$ 1.96 [g]. A typical schematic drawing of the vibration test apparatus is presented on Figure 2.3.

Over a few days the structure is subjected to about one million cycles. Every day when the test procedure is finished, the TMA is inspected for any structural damage and changes in distance between top and bottom surfaces, which could indicate failure.

2.4. Moisture Test

Other restrictions that need to be considered in order to maintain the ability of saving life is the moisture test. If the truck mounted attenuator is not capable of drainage, then excessive amount of additional weigh could result in failure.

Again, the method described by California Department of Transportation is used. In the California moisture test, the attenuator unit is sprayed twice for 24 hour in the horizontal position. After the first day it is flipped over 180 [deg]. This spray is intended to simulate 6 [in] (150 [mm]) per hour of rain. After 48 hours, the cushion is allowed to dry for 1 hour. Then the structure is disassembled and carefully examined. The test is positive only when the structure is free of moisture.

In this study, the problem is solved by introducing multiple holes both in the vertical and horizontal covers. Size of the holes is chosen so that the hole will never be blocked by any sediment or other small objects that can be encountered during TMA's lifetime.

CHAPTER 3. FATIGUE IN METALS

3.1. Overview

As mentioned in Chapter 2, one of the major serviceability problems in attenuators is damage caused by the fatigue due to vibrations of a moving carrier. It is extremely dangerous because it is usually unexpected. Destruction happens at a stress range which is far below the ultimate or yield strength of the material. In some cases, the stress failure can even occur at stress levels that are a small fraction of maximum load capacity. The process of fatigue is divided into three stages:

- **Initial -** when fatigue damage lead to crack initiation.
- **Intermediate -** propagation of a crack to a critical size (a size at which the uncracked domain is too weak to carry the loads).
- **Final -** sudden fracture of the remaining cross section.

Stress levels depend on many factors such as type of the material, heat treatment, state of the element's surface, and manufacturing technology. Also, load nature, load frequency and load duration will have direct impact on the total number of cycles to failure.

Fatigue failure can be described as a failure caused by an external load that fluctuates over the time period. Those changes can be regular, cyclical e.g. described by sinusoid.

$$F(t) = A \cdot \sin(\omega t + \varphi) \tag{3.1}$$

Where: ω is the angular frequency, φ is the phase and A correspond to the peak deviation. In such cases estimation of total number of cycles to failure is quite easy. Miner's rule should be used for

stresses that do not have constant magnitude and vary over a wide range. According to the hypothesis, failure occurs when:

$$\sum_{i}^{i} \frac{n_i}{N_i} = 1 \tag{3.2}$$

Where: n_i is the number of cycles at the *i-th* stress level and N_i described number of cycles to failure corresponding to the *i-th* stress level.

Currently, the Wohler procedure described by stress range versus number of cycles to failure (SN) curve is one of the main design parameters for the material to determine limited and permanent fatigue strength. However this law does not give any basis for the assessment of the failure evolution due to cyclic loads.

Recently the problem of estimating either the stress range below which fatigue damage will not occur or when structure has a high probability of failure due to an assumed constant load rate has become important.

In this study, fatigue problems have been considered for two common metals which are used for truck mounted attenuator – steel and aluminum. Advantages and disadvantages of those materials are discussed further in a text.

3.2. Steel

Steel is divided into eight different fatigue strengths based on “fatigue categories”. Category A corresponds to plain material. Depending on the type of mechanically fastened connection, grove welds, attachments and fillet welds are assigned to categories B to E’. For detailed description of

categories please refer to AISC Steel Design Manual or AASHTO LRFD Bridge Design Specification

From mathematical point of view fatigue resistance for steel takes form:

$$S = \left(\frac{A}{N}\right)^{\frac{1}{3}} \tag{3.3}$$

Where: S is the stress range, N number of cycles to failure and A is constant base on detail category. This constant is presented in Table 3.1

Relationship between stress range and number of cycles to failure for different categories is presented in Figure 3.1. Also constant amplitude fatigue limit threshold (CAFT) is shown there.

Detail category	***A***		**Constant Amplitude Fatigue Limit Threshold**	
	US [10^8 ksi^3]	**SI [10^8 MPa^3]**	**US [ksi]**	**SI [MPa]**
A	250	81940	24	165
B	120	39330	16	110
B’	61	19990	12	83
C	44	14420	10	69
C’	44	14420	12	83
D	22	7210	7	48
E	11	3605	4.5	31
E’	3.9	1280	2.6	18

Table 3.1 - Constants for SN curves for steel [1].

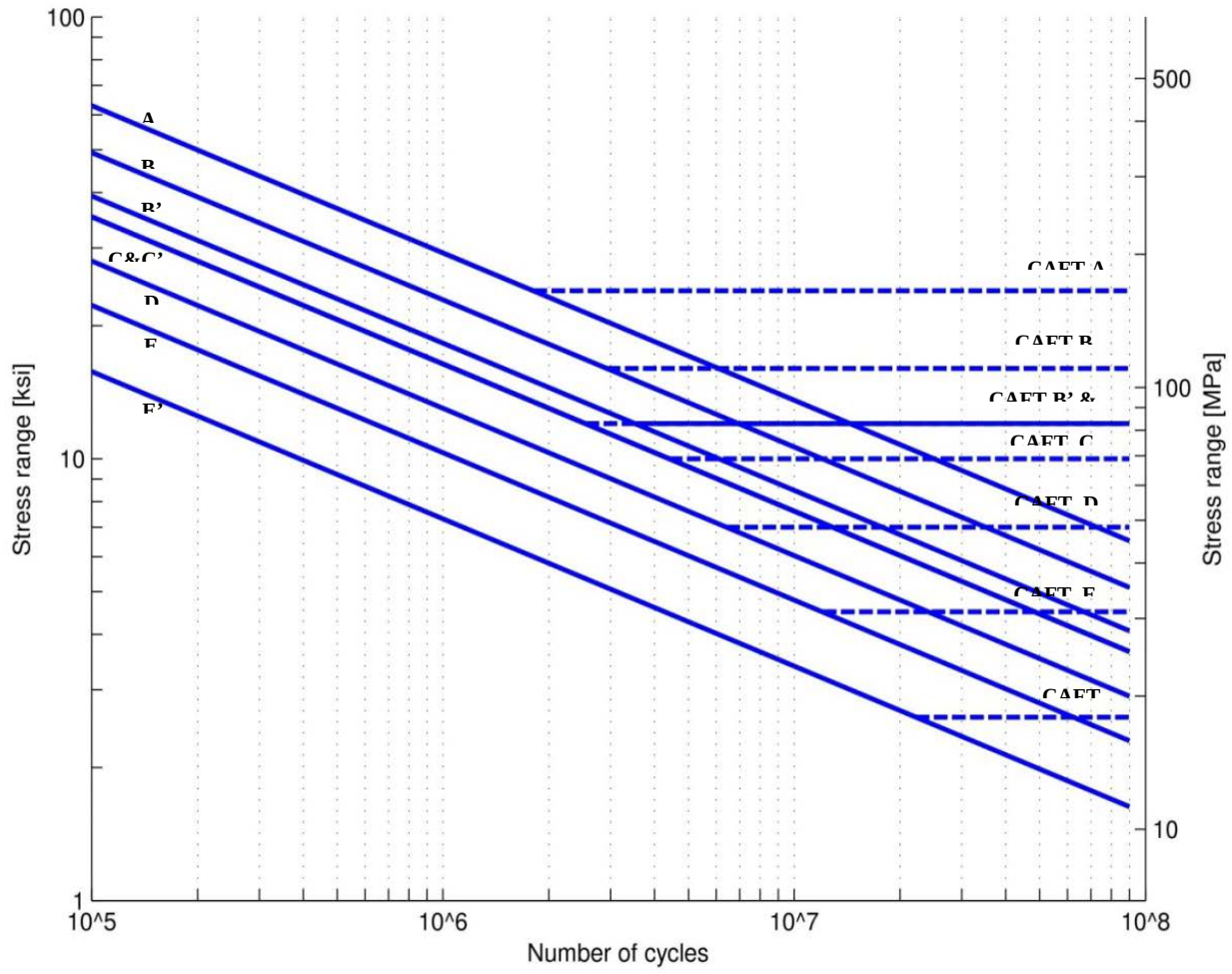

Figure. 3.1. SN curve for steel [1].

Steel is a material that demonstrates almost three times higher fatigue strength than aluminum. Whenever multiple welds are planned and the structure will be submitted to high temperatures, steel should be chosen. The only problem with the steel could be its density; aluminum weight is about three times smaller.

4)

3.3. Aluminum

The Aluminum Specification describes six different fatigue strengths based on stress categories. Category A corresponds to plain material. Depending on the type of mechanically fastened connection, grove welds, attachments and fillet welds are assigned to categories B to F. For detailed description of categories please refer to Aluminum Design Manual

Mathematically allowable stress range S is defined by:

$$S = C_f \cdot N^{\frac{-1}{m}} \tag{3.4}$$

Where: N number of cycles to failure and C_f with m are constants depending from detail category. Parameters are summarized in Table 3.3.

Not only the number of cycles, but also the stress range, and type of detail in aluminum affect the fatigue strength. Also the service temperature, weld quality, and the environmental corrosiveness are significant factors.

- Depending on the alloy's type of corrosive, the environments can decrease the fatigue strength up to one-third of the initial value. Corrosion causes damage in the material that works as crack initiation sites. This results in lower fatigue strength. Moreover electrolytic passivation process has the same effect, because it creates a brittle surface that is more vulnerable to cracking.

- Opposite to mild carbon steel, welding will reduce the strength of the alloy. This reduction depends on the type of aluminum and welding process. The critical factor is the amount of

applied heat. As a result when weld connection is being designed, not only the strength of material but the weld filler needs to be checked.

- Compared to the room temperature, whenever aluminum is submitted to extremely low temperature, fatigue strength is increased up to the order of one to two times the initial value. This happens because when the temperature decreases, tensile strength and elongation of alloy increases. Conversely, at higher temperatures fatigue strength is reduced.

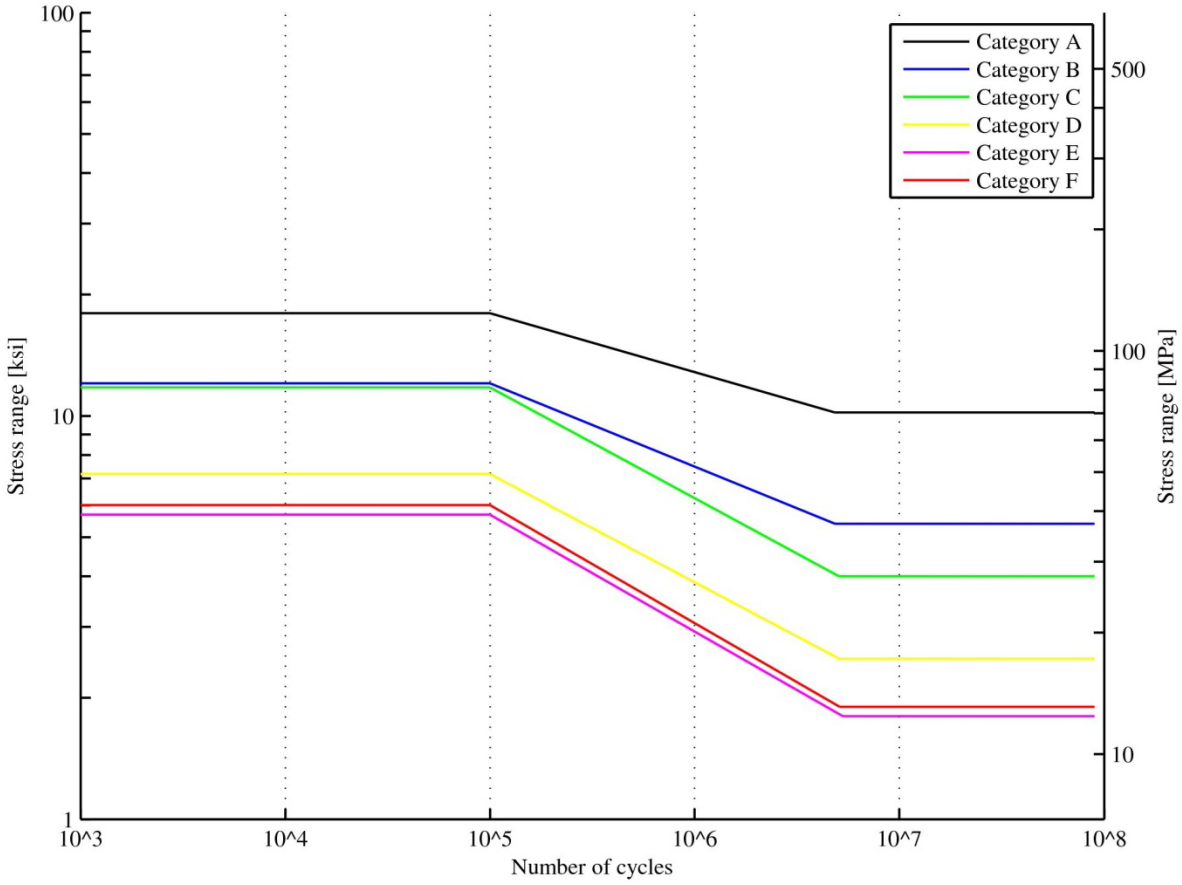

Figure. 3.2. SN curve for aluminum.

Curves presented on the Figure 3.2 are valid only for more than 10^5 cycles to failure and they are limited to stress of 80% of the material yield strength.

Detail category	C_f		m	Constant Amplitude Fatigue Limit	
	US [ksi]	SI [MPa]		US [ksi]	SI [MPa]
A	96.5	665	6.85	10.2	70
B	130	900	4.84	5.4	37
C	278	1920	3.64	4.0	28
D	157	1080	3.73	2.5	17
E	160	1100	3.45	1.8	13
F	174	1200	3.42	1.9	13

Table 3.2 - Constants for SN curves for aluminum [3].

CHAPTER 4. DEVELOPMENT OF ANALYTICAL MODEL

4.1. Introduction

To design the behavior of truck mounted attenuator basics principals of physics are used. First one is the conservation of linear momentum. Momentum of moving vehicle can be described as:

$$\overrightarrow{Momentum} = m \cdot \vec{v} \tag{4.1}$$

Where: m correspond to mass of the body and v is the velocity. Knowing that the system needs to be in equilibrium, this principal can be used to estimate the roll ahead of the truck or the decrease in speed due to sudden increase in mass of moving vehicle:

$$m_1 \cdot \vec{v}_1 = m_2 \cdot \vec{v}_2 \tag{4.2}$$

The second basic principle of physics used in the design is the principal of conservation of energy. When the nose of TMA is impacted by an errant vehicle, the vehicle is decelerated to a stop. In other words, the deformation of the cushion needs to dissipate the pre-impact kinetic energy stored in a vehicle. Indeed in this process energy is not created. Hence, the total work done in crushing of the truck mounted attenuator must be equal to initial kinetic energy of the vehicle:

$$W = KE \tag{4.3}$$

$$KE = \frac{m \cdot v^2}{2} \tag{4.4}$$

Where: W is work, KE is vehicle pre-impact kinetic energy. It is important to mention that implementation of such a principle requires a form of backup capable of resisting the impact force

applied through the collapsing of attenuator due to impacting vehicle. For TMA such a backup consists of a mobile carrier unit.

Whenever a force is applied to an object, causing the object to move, work is done by the force. If a force is applied but the object doesn't move, work is equal to zero. Work can be defined as:

$$W = \int_a^b F(s) \cdot ds \tag{4.5}$$

Where: F is force acting at point and s is distance over which the work is computed. Graphically work is equal to area under force-distance curve.

In these calculations, it is assumed that the vehicle is moving with uniformly retarded motion so the deceleration over short distance will be constant. Three equations of the motion are constitutive basis in estimations:

$$v = v_0 + at \tag{4.6}$$

$$x = v_0 + \frac{at^2}{2} \tag{4.7}$$

$$v^2 = {v_0}^2 + 2ax \tag{4.8}$$

Where: v_0 is the initial velocity, v is the final velocity, t correspond to considered time period, x is related to displacement and a describes the deceleration

4.2. Analysis Results

Analytical design is the foundation for estimation the amount of energy that needs to be dissipated at a certain distance of the cushion in order to meets the criterion described by following codes:

draft od new EN 1317 [4], MASH [5] or NCHRP 350 [6]. This TMA is intended to be used both in United States of America and United Europe. As a result differently designed vehicles have to be stopped safely. Moreover, the analytical model assumed that the truck mounted attenuator is attached to a rigid mobile carrier, so none of the advantages of roll ahead can be used. Altogether four cases have been considered for impact speed of 100 [km/h]:

- Case 1: NCHRP Report 350 [6] combined with draft of new EN 1317 [4] when all vehicles completely slowed down

- Case 2: NCHRP Report 350 [6] combined with draft of new EN 1317 [4] when the vehicles are slowed down to a certain speed. Then remaining impact force is withheld by car's stiffeners

- Case 3: MASH [5] combined with draft of new EN 1317 [4] when all vehicles completely slowed down

- Case 4: MASH [5] combined with draft of new EN 1317 [4] when the vehicles are slowed down to a certain speed. Then remaining impact force is withheld by car's stiffeners.

For the slowed down cases, only when the vehicles are not stopped completely, the movement of the mobile carrier allowed during the certification test. Moreover, the impact speed of such a vehicle will be equal to the relative speed between vehicle and moving mobile carrier. However due to fact that the first important criteria is to not exceed occupant impact velocity for different vehicles, sometimes even those cars will be slowed down completely.

Calculations were carried out assuming that the deceleration force will not exceed 18 [g] and the occupant impact velocity is not larger than 12 [m/s]. Furthermore, at the front of the attenuator additional mass is placed in a form of a steel shape. Weight of this mass is equal to about 150 [kg].

Summary of the analytical model is presented in Tables 4.1-4.18. Level of dissipated energy over the TMA length is showed on Figures 4.1-4.4.

Type	Energy [kJ]	Δ Energy [kJ]	Speed [km/h]	Distance [m]	Δ Distance [m]
pre-impact	313.4	-	100.0	-	-
steel shape	267.0	46.4	84.5	0.05	-
at OIV	125.4	141.6	57.9	1.48	1.43
stop	0.0	125.4	0.0	2.22	0.74

Table 4.1 - Summary of case 1 and case 2 for 820 kg car.

Type	Energy [kJ]	Δ Energy [kJ]	Speed [km/h]	Distance [m]	Δ Distance [m]
pre-impact	501.5	-	100.0	-	-
steel shape	449.7	51.9	89.7	0.05	-
at OIV for 820C	306.7	143.0	74.5	1.48	1.43
at stop for 820C	185.2	121.5	58.1	2.22	0.74
at OIV for 1500	167.8	17.4	55.5	2.27	0.05
stop	0.0	167.8	0.0	2.94	0.67

Table 4.2 - Summary of case 1 for 1300 kg vehicle.

Type	Energy [kJ]	Δ Energy [kJ]	Speed [km/h]	distance [m]	Δ distance [m]
pre-impact	578.7	-	100.0	-	-
steel shape	526.1	52.6	90.9	0.05	-
at OIV for 820C	387.7	138.4	78.0	1.48	1.43
at stop for 820C	262.4	125.4	64.2	2.22	0.74
at OIV	244.9	17.4	62.6	2.27	0.05
at stop for 1300C	99.5	145.4	34.8	2.94	0.67
stop	0.0	99.5	0.0	3.21	0.27

Table 4.3 - Summary of case 1 for 1500 kg vehicle.

2000 C	Energy [kJ]	Δ Energy [kJ]	Speed [km/h]	distance [m]	Δ distance [m]
pre-impact	771.6	-	100.0	-	-
steel shape	717.8	53.8	93.0	0.05	-
at OIV for 820C	580.6	137.2	83.7	1.48	1.43
at stop for 820C	455.2	125.4	74.1	2.22	0.74
at OIV for 1500C	442.4	12.9	73.0	2.27	0.05
at OIV	360.3	82.0	66.4	2.68	0.41
at stop for 1300C	270.1	90.3	57.1	2.94	0.26
at stop for 1500C	192.9	77.2	48.2	3.21	0.27
stop	0.0	192.9	42.0	3.71	0.51

Table 4.4 - Summary of case 1 for 2000 kg pickup.

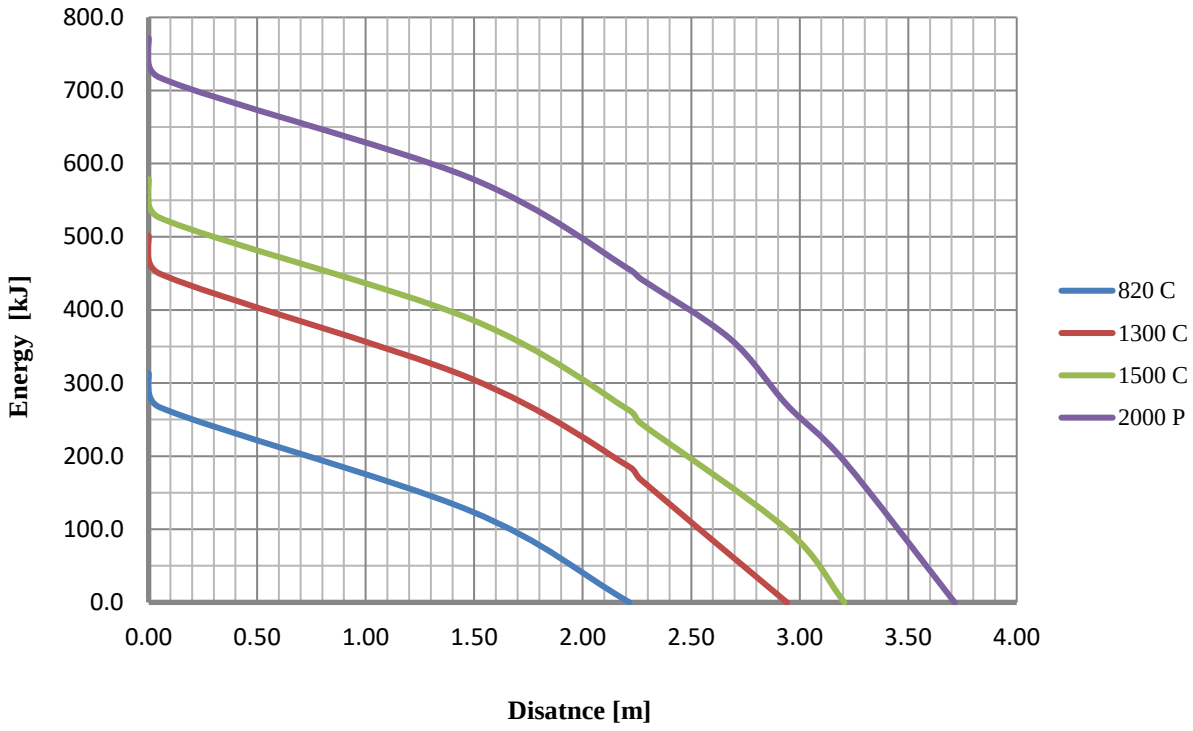

Figure. 4.1. Energy dissipation levels for case 1.

Type	Energy [kJ]	Δ Energy [kJ]	Speed [km/h]	Distance [m]	Δ Distance [m]
pre-impact	501.5	-	100.0	-	-
steel shape	449.7	51.9	89.7	0.05	-
at OIV for 820C	306.7	143.0	74.5	1.59	1.54
at stop for 820C	185.2	121.5	58.1	2.22	0.63
at OIV for 1500	167.8	17.4	55.5	2.27	0.05
slow down	22.4	145.4	20.0	2.85	0.58

Table 4.5 - Summary of case 2 for 1300 kg vehicle.

Type	Energy [kJ]	Δ Energy [kJ]	Speed [km/h]	distance [m]	Δ distance [m]
pre-impact	578.7	-	100.0	-	-
steel shape	526.1	52.6	90.9	0.05	-
at OIV for 820C	387.7	138.4	78.0	1.59	1.54
at stop for 820C	262.4	125.4	64.2	2.22	0.63
at OIV	244.9	17.4	62.6	2.27	0.05
at slow down for 1300C	99.1	145.8	39.8	2.85	0.58
slow down	25.5	73.6	20.0	3.11	0.26

Table 4.6 - Summary of case 2 for 1500 kg vehicle.

2000 C	Energy [kJ]	Δ Energy [kJ]	Speed [km/h]	distance [m]	Δ distance [m]
pre-impact	771.6	-	100.0	-	-
steel shape	717.8	53.8	93.0	0.05	-
at OIV for 820C	580.6	137.2	83.7	1.59	1.54
at stop for 820C	455.2	125.4	74.1	2.22	0.63
at OIV for 1500C	442.4	12.9	73.0	2.27	0.05
at slow down for 1300C	292.4	149.9	59.4	2.85	0.58
at slow down for 1500C	218.4	74.1	51.3	3.11	0.26
slow down	84.9	133.4	32.0	3.46	0.35

Table 4.7 - Summary of case 2 for 2000 kg pickup.

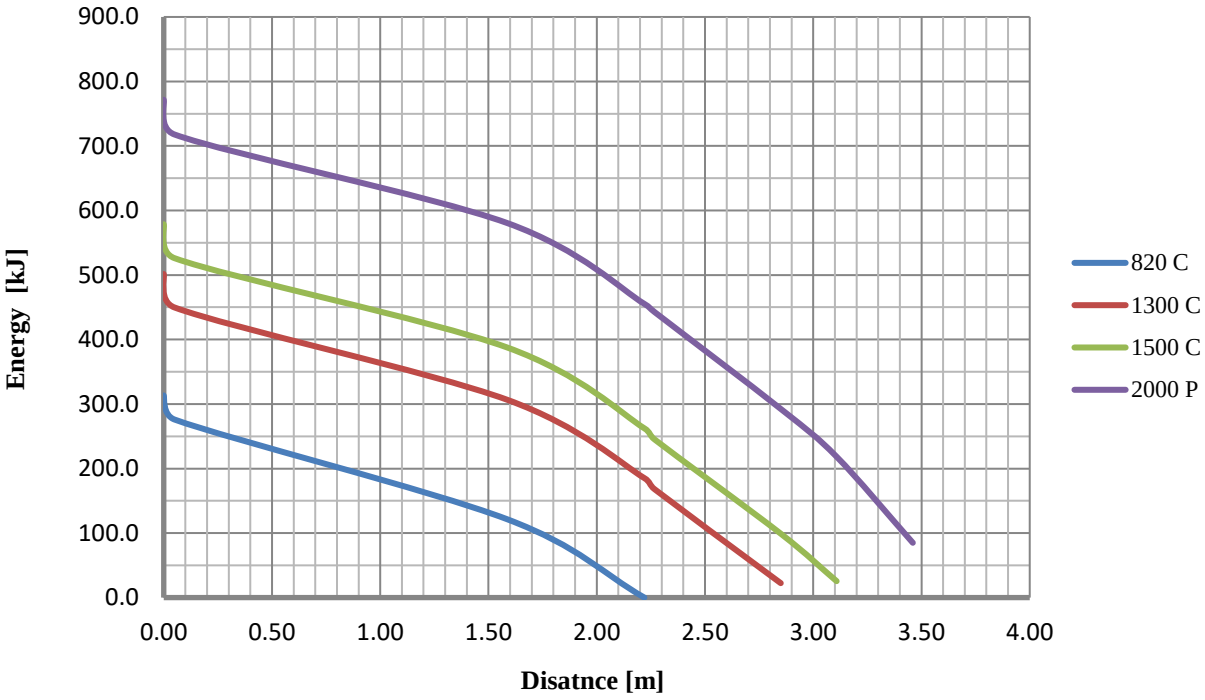

Figure. 4.2. Energy dissipation levels for case 2.

Type	Energy [kJ]	Δ Energy [kJ]	Speed [km/h]	Distance [m]	Δ Distance [m]
pre-impact	347.2	-	100.0	-	-
steel shape	297.6	49.6	85.7	0.05	-
at OIV	135.7	161.9	57.9	1.53	1.48
stop	0.0	135.7	0.0	2.26	0.73

Table 4.8 - Summary of case 3 and case 4 for 900 kg car.

Type	Energy [kJ]	Δ Energy [kJ]	Speed [km/h]	Distance [m]	Δ Distance [m]
pre-impact	424.4	-	100.0	-	-
steel shape	373.5	50.9	88.0	0.05	-
at OIV for 900C	212.9	160.6	66.4	1.53	1.48
at OIV	175.4	37.5	60.3	1.86	0.34
at stop for 900C	77.2	98.2	40.5	2.26	0.40
stop	0.0	77.2	0.0	2.61	0.35

Table 4.9 - Summary of case 3 and case 4 for 1100 kg vehicle.

Type	Energy [kJ]	Δ Energy [kJ]	Speed [km/h]	Distance [m]	Δ Distance [m]
pre-impact	501.5	-	100.0	-	-
steel shape	449.7	51.9	89.7	0.05	-
at OIV for 900C	290.0	159.6	72.0	1.53	1.48
at OIV	212.1	78.0	64.6	2.02	0.49
at stop for 900C	154.3	57.7	53.1	2.26	0.24
at stop for 1100C	77.2	77.2	37.1	2.61	0.35
stop	0.0	77.2	0.0	2.91	0.30

Table 4.10 - Summary of case 3 and case 4 for 1300 kg vehicle.

Type	Energy [kJ]	Δ Energy [kJ]	Speed [km/h]	distance [m]	Δ distance [m]
pre-impact	578.7	-	100.0	-	-
steel shape	526.1	52.6	90.9	0.05	-
at OIV for 900C	367.2	158.9	76.0	1.53	1.48
at OIV	260.9	106.3	64.0	2.19	0.66
at stop for 900C	231.5	29.5	60.3	2.26	0.07
at stop for 1100C	154.3	77.2	49.2	2.61	0.35
at stop for 1300C	77.2	77.2	34.8	2.91	0.30
stop	0.0	77.2	0.0	3.18	0.27

Table 4.11 - Summary of case 3 for 1500 kg vehicle.

Type	Energy [kJ]	Δ Energy [kJ]	Speed [km/h]	distance [m]	Δ distance [m]
pre-impact	875.8	-	100.0	-	-
steel shape	821.5	54.3	93.8	0.05	-
at OIV for 900C	664.3	157.2	84.4	1.53	1.48
at stop for 900C	528.5	135.7	57.2	2.26	0.73
at stop for 1100C	451.4	77.2	69.5	2.61	0.35
OIV/at stop for 1300C	374.2	77.2	63.3	2.91	0.30
at stop for 1500C	297.1	77.2	56.4	3.18	0.27
stop	0.0	297.1	0.0	3.87	0.70

Table 4.12 - Summary of case 3 for 2270 kg pickup.

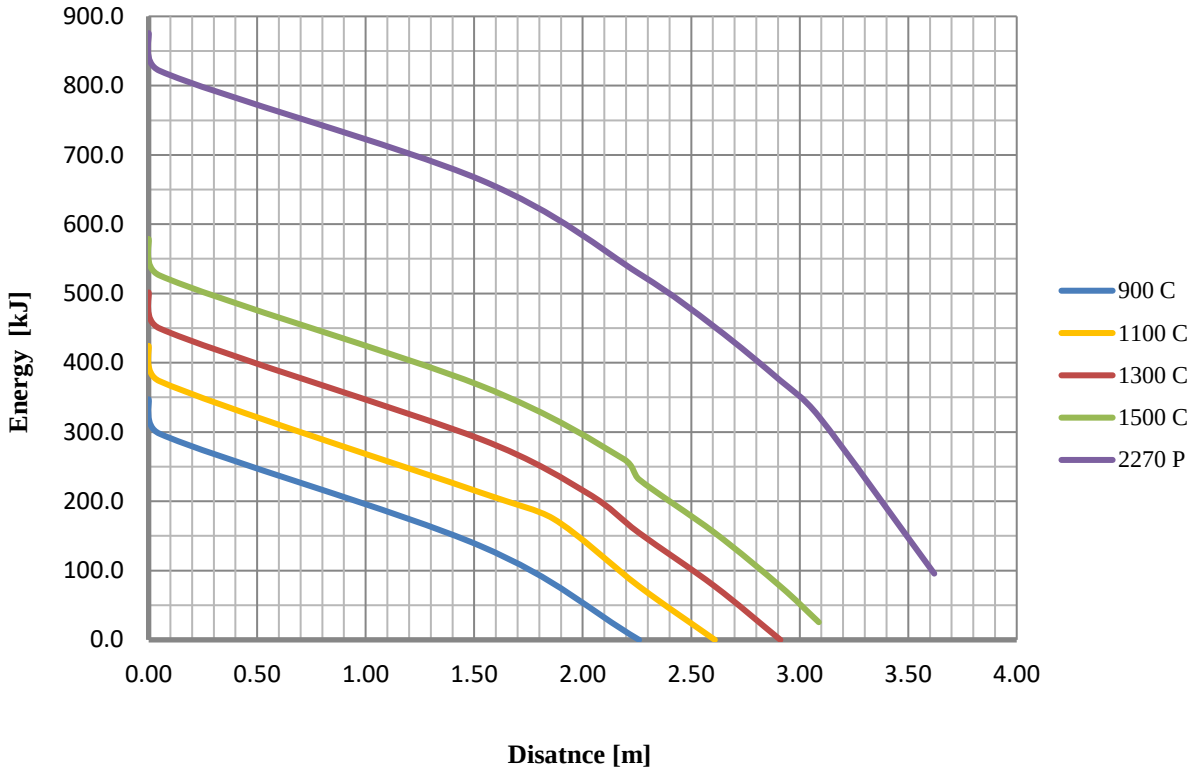

Figure. 4.3. Energy dissipation levels for case 3.

Type	Energy [kJ]	Δ Energy [kJ]	Speed [km/h]	distance [m]	Δ distance [m]
pre-impact	578.7	-	100.0	-	-
steel shape	526.1	52.6	90.9	0.05	-
at OIV for 900C	367.2	158.9	76.0	1.53	1.48
at OIV	260.9	106.3	64.0	2.19	0.66
at stop for 900C	231.5	29.5	60.3	2.26	0.07
at stop for 1100C	154.3	77.2	49.2	2.61	0.35
at stop for 1300C	77.2	77.2	34.8	2.91	0.30
slow down	25.5	51.7	20	3.09	0.18

Table 4.13 - Summary of case 4 for 1500 kg vehicle.

Type	Energy [kJ]	Δ Energy [kJ]	Speed [km/h]	distance [m]	Δ distance [m]
pre-impact	875.8	-	100.0	-	-
steel shape	831.8	44.0	95.0	-	-
at OIV for 900C	660.4	171.4	84.6	1.63	1.63
at stop for 900C	528.5	131.8	75.7	2.36	0.73
at stop for 1100C	451.4	77.2	70.0	2.72	0.36
OIV/at stop for 1300C	374.2	77.2	63.7	3.03	0.31
at slow down for 1500C	322.5	51.7	58.8	3.09	0.18
slow down	95.6	226.9	32.0	3.62	0.53

Table 4.14 - Summary of case 4 for 2270 kg pickup.

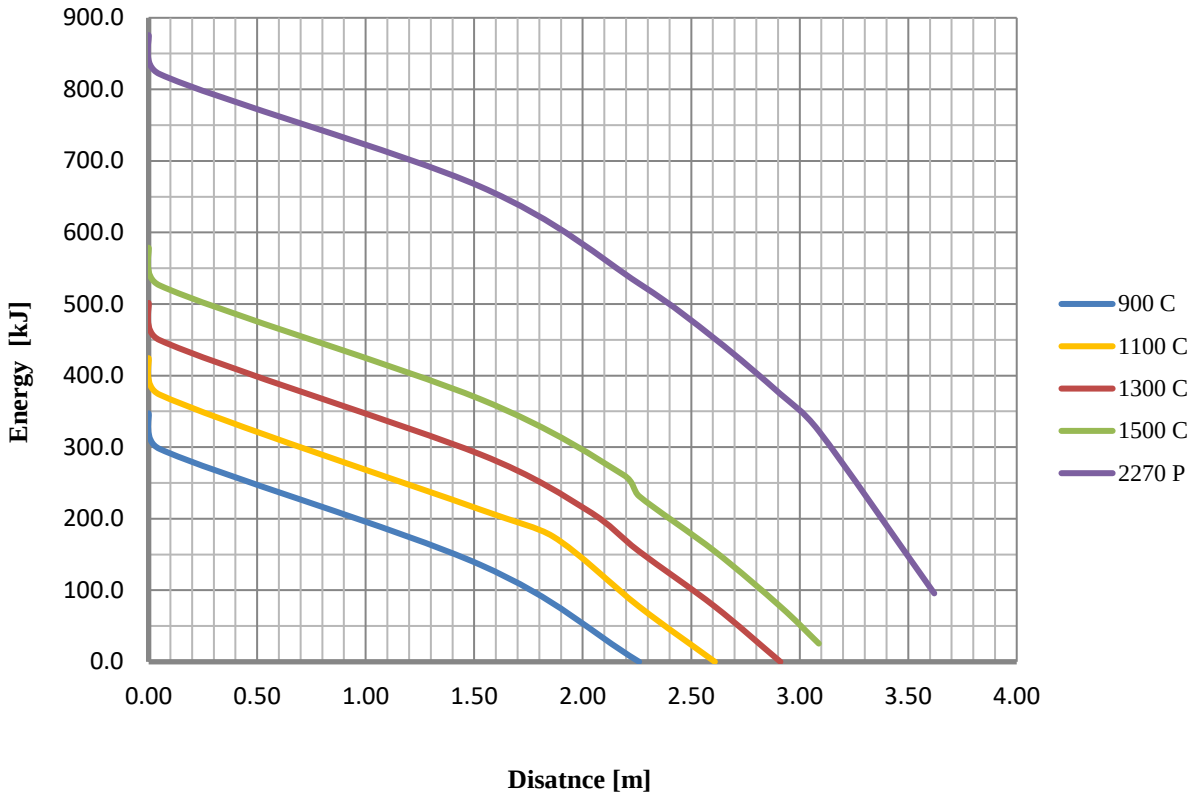

Figure. 4.4. Energy dissipation levels for case 4.

The main INTENTION OF THESE RESULTS WAS TO SHOW ONE OF THE MANY POSSIBLE LEVELS FOR ENERGY DISSIPATION FOR TRUCK MOUNTED ATTENUATOR UNDER DIFFERENT DESIGN CASES. FURTHERMORE, THEY ARE USED AS A COMPARISON BASIS FOR RESULTS OBTAINED EITHER FROM FIELD TESTS OR NUMERICAL PROCEDURE. HOWEVER, DEVELOPMENT OF TMA STRUCTURE WHICH WOULD DEMONSTRATE THE SAME BEHAVIOR AS IN ANALYTICAL PROCEDURE IS EXTREMELY DIFFICULT. THE ISSUES ARE:

- USED MATERIAL;
- DIFFERENCE BETWEEN DYNAMIC AND STATIC RESPONSE;
- PARTICULAR SHAPE OF THE ELEMENT THAT WOULD PROVIDE CONSTANT ENERGY DISSIPATION WITHOUT LARGE PEAKS ON FORCE-DISPLACEMENT CURVE. IN REALITY THIS WOULD PRODUCE AN IRREGULAR DECELERATION CURVE, WHICH IS HIGHLY NOT WELCOME;
- SHAPE OF THE ELEMENTS THAT ALLOW WOULD ALLOW MODULAR SECTION, E.G. BASED ON THICKNESS OR WIDTH;
- SPECIFIC ELEMENT CONFIGURATION IN THE STRUCTURE, SO THAT THE AMOUNT OF THE WORK DONE BY CRUSHING OF THE IMPACT VEHICLE IS CONTROLLED IN A SPECIAL MANNER SO IT CAN CORRESPOND TO ONE OF THE ANALYTICAL SOLUTIONS;
- SIMPLICITY OF THE STRUCTURE;

All of those issues have been taken under consideration.

CHAPTER 5. DEVELOPMENT OF NUMERICAL PROCEDURE

5.1. General

One of major parts of this research project is to develop a numerical model that would accurately predict the behavior of truck mounted attenuator during a vehicle impact. This inexpensive process significantly reduces the cost and number of expensive full-scale tests. Before computational power development, solution for such a problem was only available using the test-trial approach.

There are several different approaches that can be used to perform the TMA calculation. Structure components can be modeled as various types of elements. Also different solutions can be used to construct the connection between members. Moreover, the size and shape of the mesh grids can be solved in many miscellaneous ways, etc. Hence, it is very important to mention that improper modeling techniques not only increase the computational time, but it harshly affects the obtained results too. It is common to simplify numerical model at every step. Of course this requires a strong theoretical background and very good understanding of the considered problem.

Finite element analysis is performed using ABAQUS and LS-Dyna. Information provided in this chapter is mostly based on the manual, which is an integral part of the software.

5.2. Introduction to Computer Based Finite Element Analysis (FEA)

The ABAQUS Unified FEA and LS-Dyna are the most advanced software available on the market. They offers strong and complete solutions for various areas in modern engineering. They provides solution for linear and nonlinear material behavior in static and dynamic analysis. User friendly graphic interface simplifies the model building procedure and it is useful in visualizing numerical results. Indeed, it is very easy to obtain solution, however it will depend on the input data, which is why these kind of software need to be used with caution. Additionally, keyword interface and subroutine coding skills are still required in order to use the whole potential of the program.

5.3. Implicit and Explicit Method Comparison

A nonlinear analysis requires incremental steps for loading or displacements. At the end of each increment, the change in the structural geometry or material behavior may require an update in stiffness matrix for the next increment in the analysis. The solution time of the implicit solver is proportional to the square of the wave front size in the global stiffness matrix. For the explicit solver there is a linear relationship between the size of the model and the solution time, as determined by the characteristic element length and the number of elements in the model.

5.3.1. Implicit Method

In the implicit method, the state of the finite element model is updated incrementally from time t to $t + \Delta t$, based on the information at time $t + \Delta t$. There are many different procedures available in

the FE solvers, to solve this kind of problems. The most popular one is the Newton-Rawson method. For a quasi-static boundary value problem a set of non-linear equations is assembled:

$$G(u) = \int_S B^T \sigma(u) dV - \int_S N^T t dS \tag{5.1}$$

Where *G* is a set of non-linear equations, *u* is the vector of nodal displacements, *V* is the volume. *N* is the matrix with shape functions and it is integrated over the surface *S*, and *t* corresponds to the surface tractions.

Evaluations of the roots of the Eq. (5.2) are made that for the *i-th* iteration:

$$\delta u_{i+1} = u_{i+1}^{t+\Delta t} - u_i^{t+\Delta t} = -[\frac{\partial G(u_i^{t+\Delta t})}{\partial u}]^{-1} G(u_i^{t+\Delta t}) \tag{5.2}$$

Where: $u_i^{t+\Delta t}$ is the nodal displacement vector for the ith iteration at time $t + \Delta t$. Jacobian matrix of the governing equation is noted as a partial derivative on the right hand side of the equation and can be connected to stiffness matrix *K*

$$K(u_i^{t+\Delta t})\delta u_{i+1} = -G(u_i^{t+\Delta t}) \tag{5.3}$$

Finally the Eq. (5.3) must be solved in each step for incremental displacement δu_{i+1}. This procedure is quite computationally expensive. However, the time increment can be large. At this point accuracy of the solution is defined by the convergence criterion for *G*, where this value needs to be smaller than an assumed tolerance criterion. During implicit analysis, when material starts to respond with non-linear stress-strain range, many iterations are required to solve for an increment. This leads to a progressive decrease in the time step. Hence, for high nonlinear analysis it is hard to predict how long it will take to solve the problem. In some cases convergence may never occur.

Most computer based FEA software use a form of iterative Newton-Rawson method. The graphic representation of the method is showed in the Figure 5.1

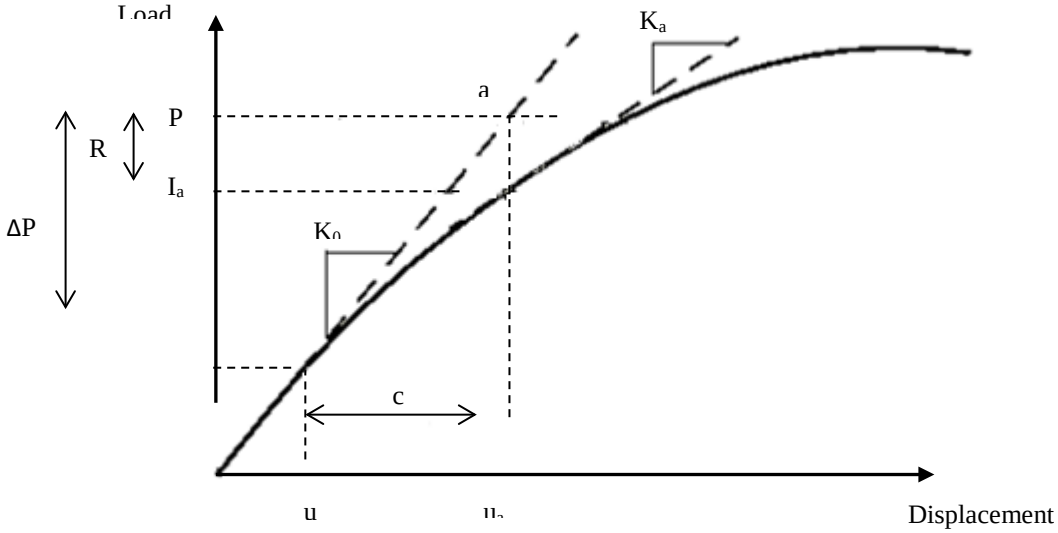

Figure. 5.1. First iteration in an iNCRement used in computer based FEA software [2].

Where: ΔP is a small load increment; K_0 is first iteration structure's tangent stiffness which is based on its configuration at u_0; K_a is the second iteration structure's tangent stiffness; c_a is the displacement correction and $I_a$correspond to structure's internal forces at updated location. If at all nodes R_a is less than assumed force residual tolerance (0.5% set by default), then computer based FEA software accepts the solution as being in equilibrium. Otherwise next iteration is performed to try to bring the internal and external forces into balance by assuming a smaller value of displacement correction.

5.3.2. Explicit Method

Whenever discontinuities are expected to occur in the model, it may be impossible to obtain an efficient solution with explicit method. A possible source of discontinuity could be impact, buckling, wrinkling, material degradation or a failure such as cracking of concrete, etc. With this approach, it is possible to achieve a smoother solution. This method has a very robust contact algorithm that does not add additional degrees of freedom to the model. Furthermore, explicit method it contains many modeling capabilities, such as material failure with element deletion for elastic-plastic materials.

In explicit methods, unknown values are obtained from the information already known. Neither convergence nor iteration checking is required. Primarily this method has been developed to solve dynamic problems involving deformable bodies. It is using an assumption saying that during the time increment accelerations and velocities are constant and they are used for solve the next point in time. Most computer based FEA software use a forward Euler scheme also known as central difference algorithm as follows:

$$u^{(i+1)} = u^{(i)} + \Delta t^{(i+1)} \dot{u}^{\left(i+\frac{1}{2}\right)} \tag{5.4}$$

$$\dot{u}^{\left(i+\frac{1}{2}\right)} = \dot{u}^{\left(i-\frac{1}{2}\right)} + \frac{\Delta t^{(i+1)} + \Delta t^{(i)}}{2} \ddot{u}^{(i)} \tag{5.5}$$

Where: u is the displacement, $\dot{u}$ is velocity, $\ddot{u}$ corresponds to acceleration and the superscripts refer to the time increment.

At the start of each increment, accelerations are computed using following expression:

$$\ddot{u}^{(i)} = M^{-1} \cdot (P^{(i)} - I^{(i)}) \tag{5.6}$$

Where: P is the vector describing the externally applied forces, I is the vector of internal element forces and M is the lumped mass matrix. For such conditions the solution is inexpensive to compute since the lumped mass matrix is diagonal matrix; the inversion process is really fast compare to global stiffness matrix, which used in the implicit solution.

Size of the time increment is described by the sTABILITy limit criteria:

$$\Delta t = \min\left(\frac{L^e}{c^d}\right) \tag{5.7}$$

$$c^d = \sqrt{\frac{\lambda + 2\mu}{\rho}} \tag{5.8}$$

Where: L^e is the characteristic element length, c^d is the dilatational wave speed, λ with μ are Lame elastic constants and ρ is the material density.

Although in the explicit method the incremental solution is easy to obtain in most cases, it may take more than 10^5 increments to finish the computations. In order to maintain the efficiency of the solution, it is important to make sure that the size of the assumed mesh gird is as regular as possible. Otherwise one small element can decrease the time increment for the whole model.

The explicit method can be used to perform quasi static analysis, but it is very impractical to use a full time scale, because runtime would be very large. However, multiple methods exist that can be used to artificially reduce the simulation time. They are divided into two groups. The first one involves a speed increase of the applied deformation or loading rate. Second involves scaling the density of the material in the model. Based on the Eq. (5.7) and Eq. (5.8), when the density is scaled by the factor α^2, the runtime is reduced by factor α. Another issue that needs to be considered is to check if the inertial forces do not affect the mechanical response, as it would provide unrealistic

dynamic results. Kutt et all [14] recommended that the ratio of the duration of the load and the fundamental natural period of the model should be greater than five in order to reduce the dynamic effect. Choi et all [10] showed that keeping the ratio of the kinetic energy to the total internal strain energy at < 5%, so dynamic effects in the model are negligible. Those criteria were used when performing quasi static analysis.

5.4. Description of Element Types

The computer based FEA software element library provides a complete geometric modeling capability. Any combination of elements can be used to create the model.

Global Cartesian coordinate system is used to identify most of the elements available in computer based FEA software. The only exceptions are axisymmetric elements, which are formulated in terms of r–z coordinates. In almost all elements, primary vector quantities such as displacements and rotations are defined in terms of nodal values with scalar interpolation functions. Element integration is performed numerically, so the virtual work integral is described by a summation:

$$\int_V \sigma : \delta D dV \rightarrow \sum_{i=1}^{n} \sigma_i : \delta D_i V_i \qquad (5.9)$$

Where: n is the number of integration points in the element and V_i is the volume associated with integration point i. FEA software will use either “full” or “reduced” integration.

5.5. Material Models

Classic metal plasticity with isotropic hardening is used to describe the stress-strain characteristic of the metals. Most computer based FEA software offers several models for the metal plasticity analysis. For this study it was assumed that the rate-independent plasticity with isotropic hardening and a von Misses yield surface will be used.

The basic assumption of the elastic-plastic models is that the deformation can be divided into an elastic part and a plastic part. Usually this statement is written in general form as a:

$$F = F^{el} \cdot F^{pl} \tag{5.10}$$

Where: F is the total deformation gradient, F^{el} is the fully recoverable part of the deformation at the point under consideration and F^{pl}corresponds to inelastic response.

Direct decomposition lead to formulation for the plastic model:

$$\dot{\varepsilon} = \dot{\varepsilon}^{el} + \dot{\varepsilon}^{pl} \tag{5.11}$$

Here $\dot{\varepsilon}$ is the total mechanical strain rate, $\dot{\varepsilon}^{el}$ is the elastic strain rate, and $\dot{\varepsilon}^{pl}$ is the plastic strain rate.

The yield function, *f*, defines the limit to this region of purely elastic response and is written so that for purely elastic response:

$$f(\sigma, \theta, H_\alpha) < 0 \tag{5.12}$$

Where: θ is the temperature, and H_α are a set of hardening parameters. Those parameter are specified when the user define a particular plasticity mode.

In the rate-independent models the yield constraints are developed, because of stress state that causes the yield function to have a positive value during inelastic flow.

$$f_i(\sigma, \theta, H_{i,\alpha}) = 0 \tag{5.13}$$

When the material is flowing inelastically the plastic part of the deformation is defined by the flow rule, which we can write as:

$$d\varepsilon^{pl} = \sum_i d\lambda_i \frac{\partial g_i(\sigma, \theta, H_{i,\alpha})}{\partial \sigma} \tag{5.14}$$

Where: $g_i(\sigma, \theta, H_\alpha)$ is the flow potential for the *i-th* system and λ_i is the rate of change of time. General plasticity models have several active flow potentials at a point.

The final ingredient in plasticity models is the set of evolution equations for the hardening parameters. We can write these equations as:

$$dH_{i,\alpha} = d\lambda_i h_{i,\alpha}(\sigma, \theta, H_{i,\beta}) \tag{5.15}$$

Where: $h_{i,\alpha}$ is the hardening law for $H_{i,\alpha}$.

Rate-independent plasticity is common for modeling the response of metals and some other materials at low temperature and low strain rates. The hardening rule is used to describe the changing of the yield surface with progressive yielding, in order to establish the conditions for subsequent yielding. Isotropic hardening is generally considered to be a suitable model for problems in which the plastic strain goes well beyond the incipient yield state and the Bauschinger effect is noticeable.

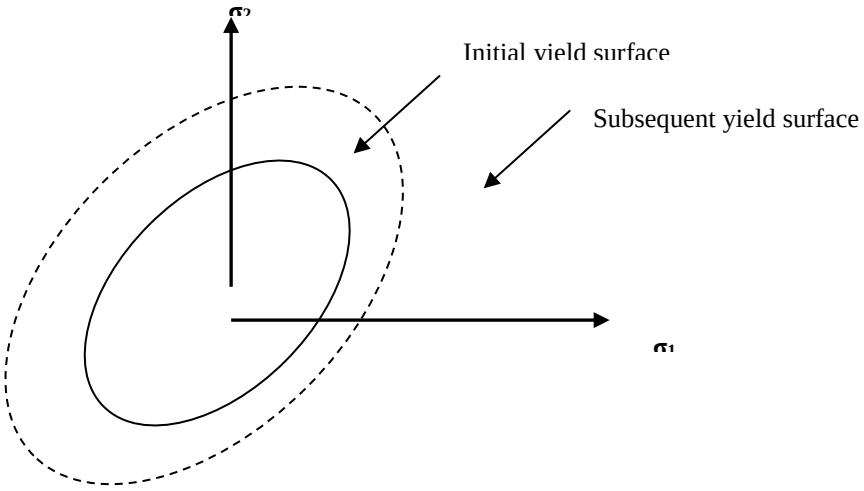

Figure. 5.2. Isotropic work hardening.

Therefore it is used for many dynamic problems where finite strains are involved or in analyzing manufacturing processes. For this hardening theory, the yield surface remains centered about its initial centerline and expand in size as the plastic strains develop. Figure 5.2 illustrates isotropic work hardening.

For this particular case the yield function is given as:

$$f(\sigma) = \sigma^0(\varepsilon^{pl}, \theta) \tag{5.16}$$

Where: σ^0 is the equivalent (uniaxial) stress, θ is temperature, ε^{pl} is the work equivalent plastic strain, defined by:

$$\sigma^0 \dot{\varepsilon}^{pl} = \sigma : \dot{\varepsilon}^{pl} \tag{5.17}$$

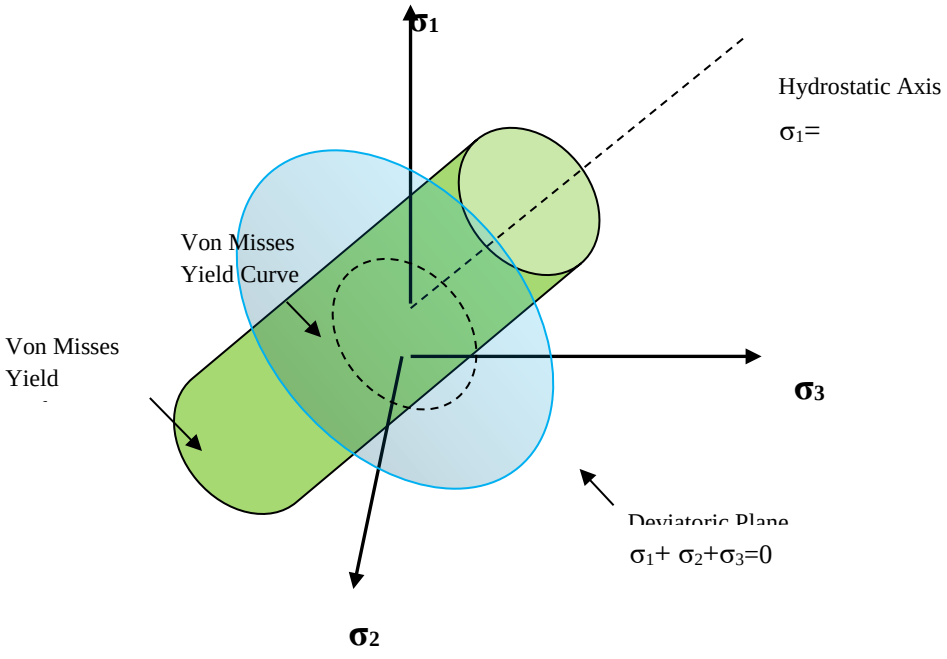

Figure. 5.3. The von Misses yield surfaces in principal stress [www.wikipedia.com].

The von Misses criterion assumes that the yielding of the material begins when the second deviator stress invariant J_2 reaches a critical value. Prior to this, the yielding material response is elastic. Due to the independence of the first stress invariant I_1, it is widely used in analysis of plastic deformation for ductile materials. In engineering, the von Misses criterion is described as:

$$\sigma_1{}^2 + \sigma_2{}^2 + \sigma_3{}^2 - \sigma_1\sigma_2 - \sigma_2\sigma_3 - \sigma_1\sigma_3 = \sigma_Y{}^2 \qquad (5.18)$$

Where: $\sigma_1, \sigma_2, \sigma_3$ are the stresses in the three principal axes and σ_Y is the yield stress. Graphic representation of failure surface for three dimensional cases is showed in Figure 5.3

Altogether four different metals were considered in the computations. Each material behavior is defined by tabulated data using true stress and corresponding to it true plastic strain. Parameters

for two aluminum types are presented in Table 5.1. Steel properties are showed in Table 5.2 and on Figure 5.4. For each of them the failure mechanism is implemented: whenever an element in the mesh grid reaches its maximum strength and its rupture occurs, then an element is deleted from the model and it is not used in any further computations. When used wisely, this operation not only gives a closer results but it has a positive impact on the total runtime of the model.

TYPE	5052 H32	5754 H22
Density [kg/m^3]	2680	2670
Modulus of Elasticity [GPa]	70.3	70.3
Poisson's Ratio	0.33	0.33
Yield Strength [MPa]	193	185
Ultimate Strength [MPa]	228	245
Elongation at break	0.12	0.15

Table 5.1 - Aluminum properties.

TYPE	S235	S355
Density [kg/m^3]	7850	7850
Modulus of Elasticity [GPa]	210	210
Poisson's Ratio	0.3	0.3
Yield Strength [MPa]	235	355

Table 5.2 - Steel properties.

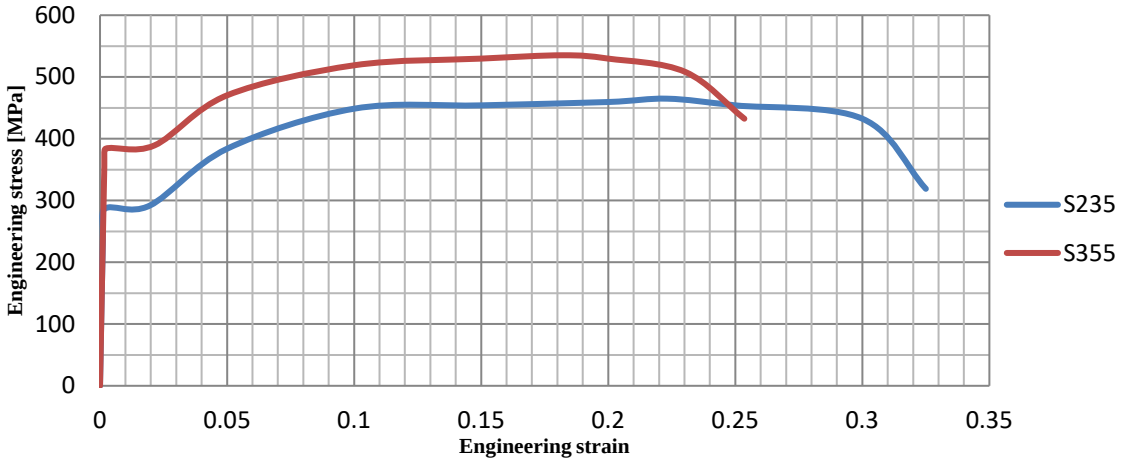

Figure. 5.4. Stress strain behavior for steel S235 and S355 [19].

CHAPTER 6. DEVELOPMENT OF ENERGY DISSIPATION METHOD

6.1. New Unique Technology

The main idea of designed TMA is inspired by an old and non-protected any more US patent 3,146,014 filled on Aug. 12 1959 - "Energy Absorbing Vehicle Bumper Assembly". The invention has as its principal object to provide an improved device of this type for absorbing energy through telescoping a tubular member axially of itself, whereby the side walls of the tube are progressively flexed or bent radially and then in a reverse axial direction along the length of the tube. Such initial bending and re-straightening of the tube side walls effects a double working of the material with consequent efficient energy absorption in terms of the length of displacement of the tube ends relative to each other. The absorption device in accordance with the invention has important advantages over others previously proposed in being relatively inexpensive to manufacture and impervious to corrosion damage in service, and in requiring no lubrication. [20]

Designed Truck Mounted Attenuator uses a C-shape 180 degree bending – a plastic deformation technology to dissipate the energy of the impacting vehicle. The basic concept is quite simple. When an engaged tube with a bar welded at the front is forced to proceed forward it start to bend fixed C-shape section by 180degrees The graphics shown in figure 6.1 illustrate this plastic deformation process.

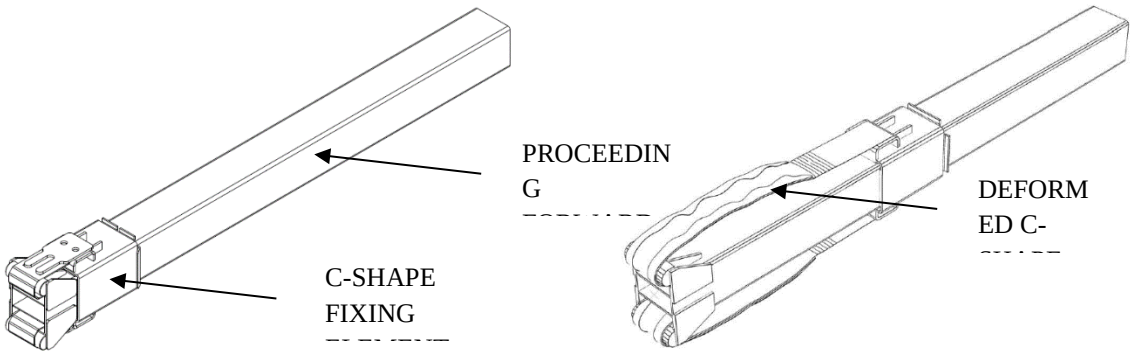

Figure. 6.1. Plastic deformation of two fixed C-shapes by proceeding forwards engaged tube.

This C shape 180deg bending process, dissipates the energy of the impacting vehicle. The level of energy dissipation can be regulated by using different thickness and dimensions of C-shape, the type of material or material grade and the diameter of the bar welded at the front of the engaged tube.

By adjusting the level of energy dissipation and the lengths of the energy absorbing C-shape, the amount of energy dissipation and the rate of vehicle deceleration can be controlled to bring the impacting vehicle to a gradual and safe stop.

Also, the 180 degree bended c-shapes are still fixed from the impacting vehicle, thus eliminating any hazard posed to the impacting vehicle. Thus there are no detached elements that can be thrown forward and pose hazard to workers and adjacent traffic.

6.2. TMA Validation - Crash Testing

Multiple crash tests have been conducted using the rigid “bogie” vehicle. The speed of the impact varied however the vehicle mass was fixed - about 2450 [kg]. All of the tests were conducted in a facility which is capable of testing road safety structures and has all necessary equipment.

The object of those tests was to obtain the decelerations data and overall behavior of the structure in order to calibrate the computer based finite element models and optimize the design. Process of field testing and calibration have to be repeated several times until all issues have been eliminated from the designed structure.

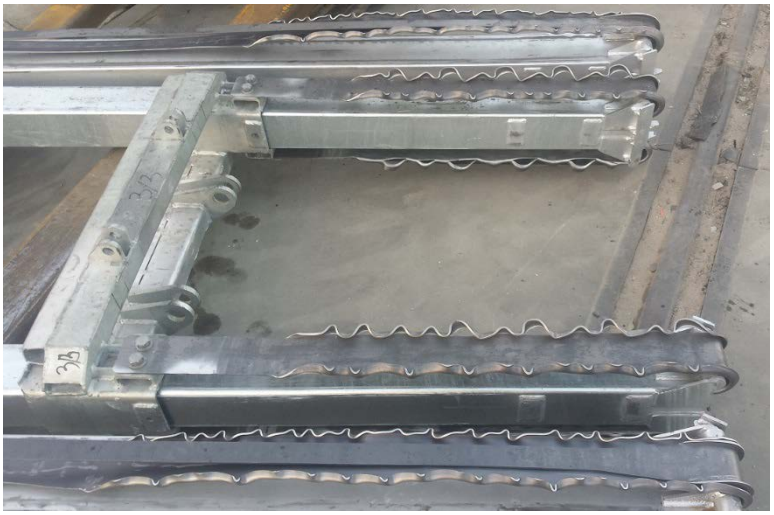

Figure. 6.2. Final design of TMA after impact of rigid bogie impact at 75 kmh.

Compliance test have been conducted at DTC Dynamic Test Center in Vauffelin, Switzerland according to NCHRP 350 Recommended Procedures for the Safety Performance Evaluation of Highway Features.

CHAPTER 7. TECHNICAL SPECIFICATION AND FABRICATION PROCESS

7.1. Technical Specification

A complete workshop documentation has been created in computer aided engineering software called Autodesk Inventor. It is a 3D mechanical solid modeling design software developed by Autodesk to create 3D digital prototypes. It is used for 3D mechanical design, design communication, tooling creation and product simulation. This software enables users to produce accurate 3D models to aid in designing, visualizing and simulating products before they are built.

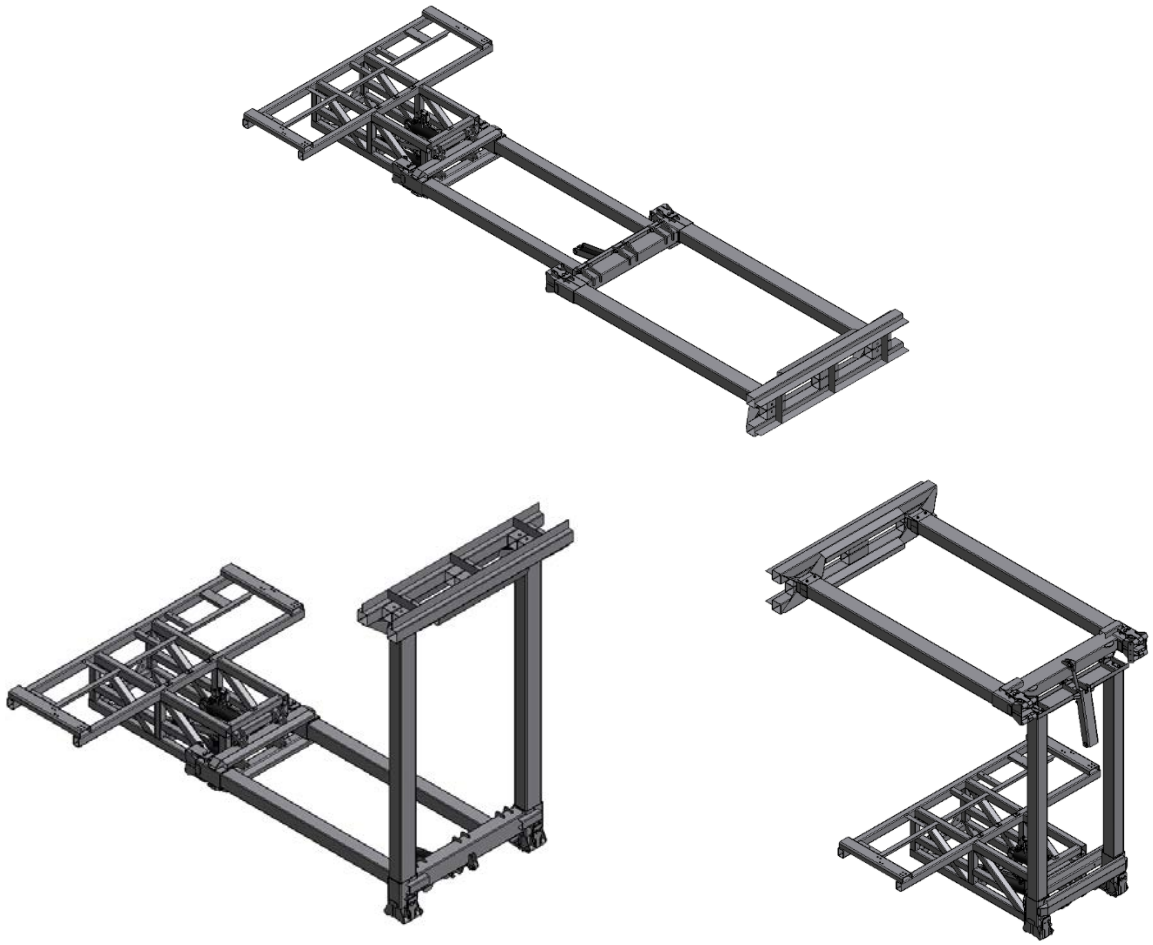

Figure. 7.1. 3D model of TMA from Autodesk Inventor in 3 positions

Overall Dimensions in impact ready:

1. Length 6050mm
2. Width 2300mm
3. Height (to top of impact head) 700mm
4. Height (to top of Docking station) 800mm
5. Ground Clearance (to bottom of impact head) 300 mm

Capacity:

1. TMA Energy Dissipation Unit 450 kg
2. TMA - Docking Station 230 kg

7.2. Fabrication

It is recommended that manufacturing process should be handled according to guidelines published in international quality management standard ISO 9001, in order to continually monitor and manage quality across all operations and to cut errors.

Manufacturing process should enable full traceability of all involved personnel and material origin. All used materials, weldments, bolted connections should be handled according to technical documentation.

In order to manufacture TMA unit independently, it is required that the workshop should have access to laser cutting system, shear blades, press brake tooling and quality welding semi-automated workbenches for steel and aluminum. 3D model developed in Autodesk Inventor use a shortcut system that recommends that method of element manufacturing. However manufacturer is free to choose different method as long as elements will keep imposed dimension deviations:

- lms – laser cutting system,
- fbs - shear blades,
- dms - press brake tooling.

Any modifications in the technical documentation showed in this research report are not allowed without receiving written permission from the author. Author will not take any responsibility in case of TMA failure, caused by manufacturing and/or assembling process, which is not in accordance with the guidelines available in this research report.

7.3. Assembling

Assembling of Truck Mounted Attenuator should be handled according to drawings from Appendix. All subassembly elements have to be hot-dip galvanized. Bolted connections should be tighten using torque showed in table 7.1

Diameter	ISO Pitch	Head Size	Tightening Torque for Bolt Grade					
			5.6	5.8	6.8	8.8	10.9	12.9
[mm]	[mm]	[mm]	[Nm]	[Nm]	[Nm]	[Nm]	[Nm]	[Nm]
6	1	10	3.53	4.95	5.6	7.5	11	12.9
8	1.25	13	8.5	11.9	13.6	18.2	26	31
10	1.5	16	16.8	23	27	36	52	61
12	1.75	18	29	40	46	62	91	106
14	2	21	46	65	74	99	145	170
16	2	24	71	100	115	153	225	263
18	2.5	27	99	139	159	220	313	366
20	2.5	30	140	196	225	311	440	515
22	2.5	34	192	269	307	424	602	704
24	3	36	241	338	387	534	758	887
30	3.5	46	483	677	773	1 067	1 515	1 773
36	4	55	841	1 177	1 346	1 855	2 636	3 085

Table 7.1 - Tightening Torque for Bolts

7.4. Optional equipment

Depending on governing laws and regulation or customer requirements, there might be a need to include additional equipment to the Truck Mounted Attenuator (e.g. warning board, battery box, etc). Those elements were not a part of this research project.

In order to maintain integrity with TMA during the impact, design of any new optional equipment should additionally include scenario when a force of 5[g] is acting on whole body and all connecting elements – bolts/welds.

REFERENCES

[1] "AASHTO LRFD Bridge Design Specifications", American Association of State Highway and Transportation Officials, Washington D.C., 2010.

[2] "ABAQUS Documentation", Dassault Systèmes, 2011.

[3] "Aluminum Design Manual", The Aluminum Association, 2010.

[4] "DRAFT EN 1317 Road Restraint Systems", European Standard, 2013.

[5] "Manual for Assessing Safety Hardware", American Association of State Highway and Transportation Officials, 2009.

[6] "NCHRP Report 350: Recommended Procedures for the Safety Performance Evaluation of Highway Features", Transportation Research Board, National research Council, 1992.

[7] "Procedures and Equipment for Conducting Vibration and Moisture test on Truck Mounted Attenuators", Texas Transportation Institute, 1991.

[8] Belingardi G., Obradovic J., "Design of the Impact Attenuator for a Formula Student Racing Car: Numerical Simulation of the Impact Crash Test", Journal of the Serbian Society for Computational Mechanics. 1 (4) (2010), 52-65.

[9] Carney III J.F., Chatterjee S, Albin R.B., "Development of a 100-km/h Reusable High-Molecular Weight/High-Density Polyethylene Truck-Mounted Attenuator" Transportation Research Record: Journal of the Transportation Research Board, 1647 (1998), 75-88.

[10] Choi H.H., Hwang S.M., Kang Y.H., Kim J., Kang B.S., "Comparison of Implicit and Explicit Finite-Element Methods for the Hydroforming Process of an Automobile Lower Arm" The International Journal of Advanced Manufacturing Technology 20 (6) (2002), 407-413.

[11] Griffin L.I., Zimmer R.A., Campise W.L., Mak K.K., "An Evaluation of selected Truck Mounted Attenuators with recommended Performance Specifications", Texas Transportation Institute, Texas A&M University, College Station, Texas 1990.

[12] Harewood F.J., McHugh P.E., "Comparison of the implicit and explicit finite element methods using crystal plasticity" Computational Materials Science 39 (2007) 481–494.

[13] Kissell J.R., Ferry R.L., "Aluminum Structures: A Guide to Their Specifications and Design", 2nd editon, Wiley 2002.

[14] Kutt L.M., Pifko A.B., Nardiello J.A., Papazian J.M., "Slow-dynamic finite element simulation of manufacturing processes", Computers & Structures 66 (1) (1998) 1–17.

[15] Michie J.D., "Performance and Operational Experience of Truck-Mounted Attenuators," NCHRP Project 20-5, Topic 2201, Dynatech Engineering, INC.

[16] Nia A.A., Nejad K. F., Badnava H., Farhoudi H.R., “Effects of buckling initiators on mechanical behavior of thin-walled square tubes subjected to oblique loading”, Thin-Walled Structures 59 (2012) 87–96.

[17] Du Bois P., Chou C.C., Filea B.B., Khalil T.B., King A.I., Mahmood H.F., Mertz H.J., Wismans J., “Vehicle Crashworthiness and Occupant Protection”, American Iron and Steel Institute, 2004.

[18] Sedlacek G. “High Strength Steels in Steel Construction”, Institute of Steel Construction RWTH Aachen, 2002.

[19] Kroell Charles K., “Energy Absorbing Vehicle Bumper Assembly”, US Patent 3,146,014 filed on Aug. 12, 1959

[20] “LS-DYNA User's Manual” Livermore Software Technology Corporation (LSTC), 2007.

APPENDIX